

*Full Length Research Paper*

# Properties of high calcium wood ash and densified silica fume blended cement

Cheah Chee Ban\* and Mahyuddin Ramli

School of Housing, Building and Planning, University Sains Malaysia, 11800 Penang, Malaysia.

Accepted 05 October, 2011

Recycling industrial waste material as construction material to minimize production of ordinary Portland cement could solve arising industrial waste management problems and increase environmental sustainability. This study focused on the incorporation of wood biomass ash in combination with silica fume in blended cement. In this study, physical and chemical properties of high calcium wood ash (HCWA) and densified silica fume (DSF) were thoroughly characterized. Results indicated that HCWA is an active hydraulic binder material as it is rich in calcium carbonate and quicklime content. Fresh concrete properties showed HCWA-DSF blended cement pastes have marginally higher standard consistency and significantly longer setting times as compared to pure cement paste. Additionally, hard concrete properties, such as mechanical strength, water absorption, air permeability and chloride resistance properties of mortar were also investigated. Enhancement in the compressive and flexure strength of mortar was observed for mortar mixes containing DSF and HCWA. The incorporation of HCWA at level of cement replacement ranging between 4 to 12% in combination with 7.5% of DSF was observed to significantly improve the chloride resistance of mortar mixes produced.

**Key words:** High calcium wood ash, ternary blended cement, mechanical strength, durability, recycling.

## INTRODUCTION

The use of wood biomass as a source of renewable energy is gaining its popularity among the timber product industry and power production sector in several developed countries. Though having scarce fossil fuel resources this is especially common for countries such as Portugal and Spain. The greatest potential for long term cost savings with the use of wood biomass energy and low level emissions are the main reasons supporting the development of several full scale wood biomass power plants in these countries. This allows them to supplement the electrical energy demand of their national electrical gridlines. Moreover, the consumption of wood wastes

derived from the local logging and timber processing activities as fuel in the wood biomass power plant serves as the ultimate solution to solid waste management problems related to the aforementioned waste materials.

A major problem related to electrical power production using a wood biomass power plant is the formation of significant amount of wood waste fuel ash as by-product. This normally occurs at the end of the thermal conversion process. In the absence of proper disposal technique, the fine and light weight wood ash produced poses serious air pollution and health hazards to humans. Therefore, the reuse of wood ash as a supplementary binder material in concrete is perceived as a viable and sustainable method for disposal of the waste in mass amounts without side effects to the environment.

In modern civilization, structural concrete is the most common construction material with an annual consumption of approximately 10 billion tonnes (Yaprak et al., 2011). In conjunction with contemporary development in material science, ordinary Portland cement is widely used as the main constituent in concrete. The cement

\*Corresponding author. E-mail: [volrath15@hotmail.com](mailto:volrath15@hotmail.com). Tel: +60 0164846502. Fax: +60 046576523.

**Abbreviations:** HCWA, high calcium wood ash; DSF, densified silica fume; XRD, X-ray diffraction pattern; XRF, X-Ray Fluorescence; ASTM, American Society of Testing Materials; LOI, loss on ignition; CP, cement paste; C-S-H, calcium silicate hydrate; OPC, ordinary Portland cement; PC, Portland cement.

production industry currently contributes about 5% of the global anthropogenic carbon dioxide emission. Carbon dioxide is mainly emitted from the calcinations process of limestone and combustion of fuel in the kiln. Moreover, the cement production industry is also ranked third highest as a world energy consumer which contributes 19.7% of the global industrial energy consumption (Kolip and Savas, 2010). On the average, for every tonne of ordinary Portland cement produced, approximately 222 kg of carbon dioxide is generated and discharged into the atmosphere which contributes to serious environmental deterioration (Worrell et al., 2001). Hence, continuous attempts are being made (i) to reduce the cost of production of Portland cement, (ii) to reduce the consumption of the fuel and raw materials, (iii) to protect the environment and (iv) to enhance the overall quality of cement. One noted solution is to use certain low cost or waste materials for partial replacement of Portland cement. Low cost materials used are industrial and agricultural by-products (wastes). Mixture of Portland cement and the above by-products are known as 'blended cements' or 'composite cements' (Dwivedi et al., 2006). The implementation of wood ash as a supplementary hydraulic binder material in the production of blended cement concrete can be perceived as one measure to minimize the global cement consumption rate. This in turn, lowers the rate of carbon dioxide emissions from the cement and concrete production sectors.

X-ray Fluorescence (XRF) analysis performed by several researchers (Elinwa and Ejeh, 2004; Elinwa and Mahmood, 2002; Udoeyo and Dashibil, 2002; Udoeyo et al., 2006; Wang et al., 2008a) found significant amounts of silica in the ash samples obtained from incinerated wood waste. A total chemical composition of pozzolanic essential compounds, namely silica, alumina and ferric, was reported to have a range of 62.14 to 80.67% with a mean value of 72.78% which is similar to those of class N and F coal fly ashes. A published research article (Naik et al., 2003) indicated wider ranges of a total chemical composition of silica, alumina and ferric compounds between 18.6 and 59.3% for the wood ash samples examined. Recent compilation of chemical composition analysis data of ashes derived from the combustion of 28 variety of woody biomass. This indicated a high mean calcium oxide composition (43.03%) with certain types of woody biomass ash having a calcium oxide content up to 83.46% of total mass of ash (Vassilev et al., 2010). The reported findings justify that wood biomass ash may possibly contain a high calcium oxide composition which may render it hydraulically reactive. The exposure of wood ash to high temperatures of 800 to 950°C during incineration of wood biomass may result in partial decomposition of calcium carbonate composition which occurs at a temperature range of 615 to 775°C, forming quicklime (CaO) minerals. A study performed to investigate the interaction between quicklime and siliceous materials (fly ash) in quicklime-fly ash blended cement,

and concluded that the addition of quicklime in fly ash concrete resulted in a notable acceleration of the fly ash degree of hydration at any given curing time (Antiohos et al., 2005; Antiohos et al., 2006).

The inclusion of wood waste ash as a partial cement replacement material in wood waste ash/ordinary Portland cement (OPC) blended cement resulted in a delay of cement setting. This revealed the need for longer initial and final setting times of blended cement paste. The effects of setting time delays become more significant with the increase in the levels of cement substitutions with wood waste ash (Elinwa and Ejeh, 2004; Elinwa and Mahmood, 2002; Udoeyo and Dashibil, 2002). At the level of cement replacement with wood waste ash up to 30% by total binder weight, both the initial and final setting times of the blended cement paste are still in compliance to the limits prescribed in the standard code of practice BS 12: 1978 (Udoeyo and Dashibil, 2002).

Several researchers (Elinwa and Ejeh, 2004; Elinwa et al., 2008; Elinwa and Mahmood, 2002; Udoeyo and Dashibil, 2002) had common findings that show the use of wood waste ash as a partial cement replacement material in concrete at all levels of cement replacement between the range 5 and 30%. This reduces the compressive strength of the concrete mix produced relative to neat OPC concrete for all curing times. The trend observed is most probably due to the mechanism that wood waste ash particles act more like filler material within the cement paste matrix than as binder material. Thus, increasing ash content as a replacement of cement resulted in an increased surface area of filler material to be bonded by decreasing the amount of cement which caused a decline in strength (Udoeyo et al., 2006). However, a marginal difference of compressive strength between wood waste ash concrete and neat OPC control concrete mix was observed. This marginal difference tends to decrease with prolonged curing durations, especially beyond 28 days. This observation is evidence of increased calcium silicate hydrate (C-S-H) gel formation within cement paste matrix microstructure of wood waste ash concrete by pozzolanic activity (Udoeyo and Dashibil, 2002).

Wang et al. (2008a) investigated the chloride penetration resistance of air entrained concrete mix with a partial replacement of cement binder using wood fly ash and wood/coal blended fly ash. Particular levels of cement replacement by several types of fly ash were maintained at 25% total binder weight. Various types of fly ash used as a partial cement replacement material were, to name a few, combustion of wood (Wood), class C coal/wood blended fly (Wood C), class F coal/wood blended fly ash (Wood F), class C and class F coal fly ash and fly ash from co-combustion of coal and switch grass (SW1 and SW2). Wood C and Wood F blended fly ash were produced by blending class C and class F coal fly ash with pure wood ash at a mass ratio of 80% coal fly

ash and 20% wood waste fly ash. Test results indicated that (i) the incorporation of wood waste ash at a cement replacement level of 25% in air entrained concrete mix did not result as a significant impairment of the chloride permeability property of concrete. (ii) The utilization of wood waste/class F coal blended fly ash in a partial substitution of cement had a significant contribution towards lowering of the chloride permeability property of concrete mix.

Although there has been a substantial amount of work performed to investigate the properties of high silica wood ash blended cement paste, very little research was done to study the properties of high calcium wood ash and its blended cement paste.

This study was performed with the main objective to investigate the viability of the incorporation of high calcium wood ash (HCWA) in combination with densified silica fume (DSF) as a supplementary hydraulic binder in a ternary blended cement system. Throughout the study, both high calcium wood ash and silica fume were thoroughly characterized in terms of their respective particle size distribution, specific surface area, chemical composition and mineralogy phases in order to assess its suitability for use as supplementary hydraulic binder. Following that, the engineering properties of HCWA-DSF blended cement, namely, standard consistency, initial setting time and final setting time were determined. In addition the mechanical strength and chloride resistance of mortar mixes containing HCWA-DSF blended cement was also investigated.

## MATERIALS

### Portland cement (PC)

American Society of Testing Materials (ASTM) Type I Portland cement (PC) with median particle size of 3.9  $\mu\text{m}$ , specific surface area of 1.0432  $\text{m}^2/\text{g}$  and specific gravity of 3.02 were used in this study. Both the physical and chemical properties of cement used complied with specifications in ASTM Standard C150 (ASTM, 1997a; Ye et al., 2007). The chemical composition of PC used is presented in Table 1.

### High calcium wood ash (HCWA)

HCWA is a by product acquired from an industrial scale fully automatic boiler unit (commercially known as Bio-Turbomax boiler) used in the rubber wood timber product manufacturing industry. The wood biomasses used as fuel in the boiler were derived from local rubber wood species dominantly *Hevea brasiliensis*. The wood biomasses were incinerated under a self sustained burning condition within an atmosphere with a turbulent air flow supplied by an in-built air pump unit. The temperature of incineration was maintained within the range of  $800\pm 10^\circ\text{C}$ . Raw wood ash extracted from the boiler unit was sieved through a laboratory sieve with an opening size of 150  $\mu\text{m}$  to remove large agglomerated ash particles and carbonaceous materials. Ash passing the 150  $\mu\text{m}$  sieve was then ground in a ring mill until a fine mean particle diameter ( $d_{50}$ ) of 8.39  $\mu\text{m}$  material was attained. The chemical compositions of HCWA are presented in Table 1.

Particle grading curves of binder materials namely, HCWA, DSF and PC are presented in Figure 1. Median particle size of ground HCWA was found to be 8.39  $\mu\text{m}$  with a corresponding specific surface area of 611.0  $\text{m}^2/\text{kg}$  as compared to the PC sample which had a median particle size of 6.14  $\mu\text{m}$  and specific surface area of 1123.3  $\text{m}^2/\text{kg}$ . The observations were in close agreement with the fact that the median particle diameter of a powder material is inversely proportional to its specific surface area. In addition, the particle size distribution curve indicates a close resembling particle size distribution between HCWA and PC within the range of 10 to 150  $\mu\text{m}$ . However, for particles with size ranging between 0 to 10  $\mu\text{m}$ , HCWA particles were generally coarser as compared to the PC particles. The specific gravity of ground HCWA particles was determined to be 2.52.

The results of X-ray fluorescence analysis on HCWA, DSF and PC are presented in Table 1. From the test results, it can be observed that the major oxide compounds present in HCWA are CaO, MgO and  $\text{K}_2\text{O}$  which comprise 61, 8.7 and 12% of the total mass, respectively. Large compositions of CaO of the ash indicates that the ash could be hydraulically reactive (Rajamma et al., 2009). A significant amount of  $\text{K}_2\text{O}$  present is indicative that HCWA has a high level of alkalinity. Other substances namely Cl,  $\text{TiO}_2$ , MnO,  $\text{Rb}_2\text{O}$  and  $\text{Al}_2\text{O}_3$ ,  $\text{SiO}_2$ ,  $\text{P}_2\text{O}_5$ ,  $\text{SO}_3$ ,  $\text{Fe}_2\text{O}_3$ , CuO were detected in minor quantities. The loss on ignition of HCWA was found to be 18%. The significant loss on ignition of HCWA is probably due to partial thermal decomposition of calcium carbonate phases into calcium oxide followed by the release of carbon dioxide at the test temperature ( $750^\circ\text{C}$ ) (Zelic et al., 2000).

The X-ray diffraction pattern (XRD) of HCWA is shown in Figure 2. A careful analysis of this pattern indicated that the major chemical phases of the HCWA were calcium carbonate ( $\text{CaCO}_3$ ) and Portlandite ( $\text{Ca}(\text{OH})_2$ ). Calcium carbonate mineralogical phase, when used as supplementary binder in conjunction with Portland cement, may act to accelerate the hydration rate of the  $\text{C}_3\text{S}$  mineralogical phase which is present in Portland cement (Kakali et al., 2000; Lothenbach et al., 2008). The mechanism is beneficial for rapid strength gain of cementitious mix containing HCWA at early age of hydration. In addition, HCWA which is rich in the mineral and Portlandite, can be suitably used in combination with silica rich powder material such as silica fume. An early dosage of Portlandite is used to accelerate the formation of C-S-H gel by a secondary hydration reaction. The presence of these chemical phases is in close agreement with the results of X-Ray fluorescence analysis as shown in Table 1. This is indicative of the presence of significant quantities of CaO (61%) within HCWA.

### Densified silica fume (DSF)

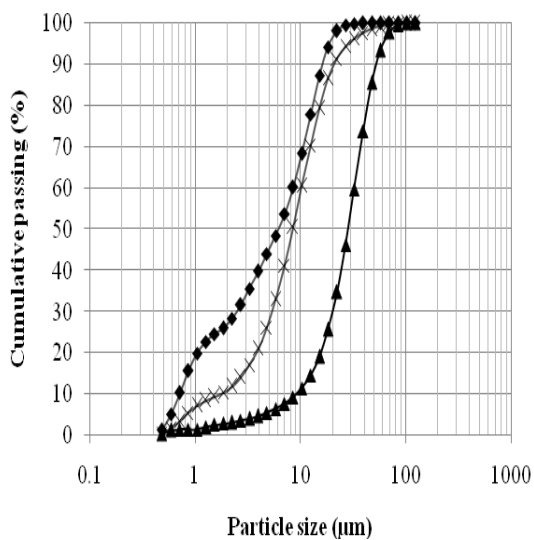
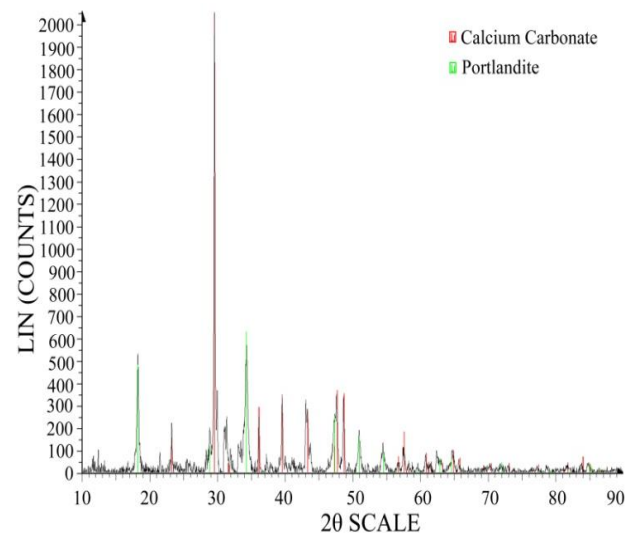
Silica fume used in this study was collected from the precipitator unit of local industrial ferrosilicon after it had undergone densification process for enhancement of its bulk density. Densification of raw silica fume was carried out by the air flotation method within the storage silo for a 24 h period. At the end of the densification process, particle agglomerates with size ranging between 10 and 1000  $\mu\text{m}$  were formed. Results obtained from laser particle diffraction analysis indicated that DSF used in the study had a median particle size of 28.21  $\mu\text{m}$  and specific surface area of 0.2170  $\text{m}^2/\text{g}$ . The specific gravity of DSF was determined to be 2.28. The chemical composition of DSF used is summarised in Table 1.

The median particle diameter and specific surface area of DSF were determined to be 28.21  $\mu\text{m}$  and 217.0  $\text{m}^2/\text{kg}$ , respectively. Particle grading of DSF particles is significantly coarser as compared to both HCWA and PC particles. The observation is consistent with the findings of other researchers (Yajun and Cahyadi, 2003) and serves as further evidence that the densification of silica fume results in agglomeration of silica fume clustered

**Table 1.** Chemical compositions and physical properties of Portland cement, HCWA and DSF.

Chemical compound	% by total mass		
	Portland cement (PC)	High calcium wood ash (HCWA)	Densified silica fume (DSF)
MgO	1.500	8.700	4.600
Al <sub>2</sub> O <sub>3</sub>	3.600	1.300	0.270
SiO <sub>2</sub>	16.000	2.700	84.000
P <sub>2</sub> O <sub>5</sub>	0.057	2.700	0.050
SO <sub>3</sub>	3.100	2.800	0.440
Cl	n/d	0.100	2.400
K <sub>2</sub> O	0.340	12.000	2.700
CaO	72.000	61.000	0.660
TiO <sub>2</sub>	0.170	0.110	0.085
MnO	0.028	0.860	n/d*
Fe <sub>2</sub> O <sub>3</sub>	2.900	1.300	0.540
NiO	n/d	trace	n/d
ZnO	trace	0.100	0.100
SrO	0.035	0.220	n/d
ZrO <sub>2</sub>	0.018	n/d	n/d
PbO	0.012	trace	0.011
CuO	n/d	0.014	trace
Rb <sub>2</sub> O	trace	0.052	0.015
C	n/d	6.700	n/d
Na <sub>2</sub> O	n/d	n/d	4.200
<b>Specific surface</b>			
Area (m <sup>2</sup> /g)	1.0432	0.611	0.217
Loss on ignition (%)			
	2.53	18.00	4.03
Median particle diameter, d <sub>50</sub> (μm)			
	6.14	8.39	28.21

\*n/d indicates that the given compound was not detected in the sample.

**Figure 1.** Particle size distribution curve.**Figure 2.** XRD patterns of HCWA.

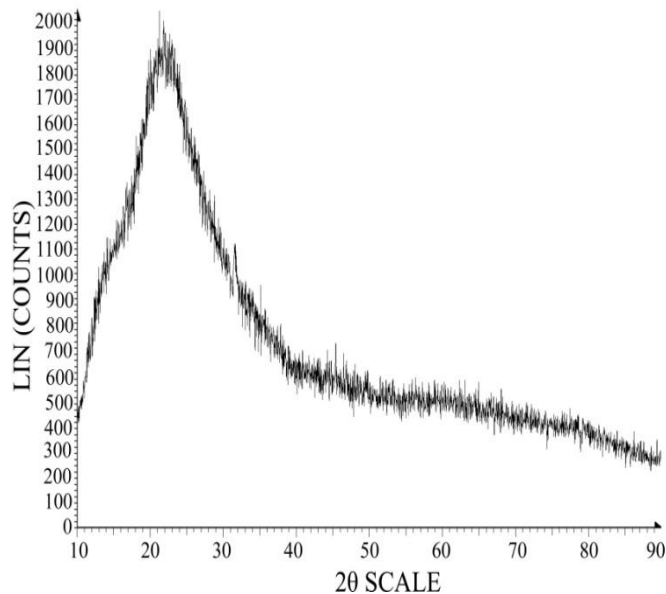


Figure 3. XRD patterns of DSF.

particles forming large diameter agglomerates. By using the laser diffraction surface area measurement technique, the measured specific surface area of DSF is the specific surface area of silica fume agglomerates. This tended to compare less than the lower limit of  $15 \text{ m}^2/\text{g}$  prescribed in ASTM Standards C1240 (ASTM, 2004c; Poppe and De Schutter, 2005).

The results of X-ray fluorescence analysis on DSF indicated that the dominant oxide compound present in DSF is silica. This constitutes 84% by total mass of the material. The other oxide compounds namely MgO,  $\text{Al}_2\text{O}_3$ ,  $\text{SO}_3$ , CaO,  $\text{Fe}_2\text{O}_3$ ,  $\text{Na}_2\text{O}$ ,  $\text{P}_2\text{O}_5$ , Cl,  $\text{K}_2\text{O}$ ,  $\text{TiO}_2$ , ZnO and PbO were detected in minor compositions as indicated in Table 1. The sum of compositions of essential pozzolanic oxide namely  $\text{SiO}_2$ ,  $\text{Al}_2\text{O}_3$  and  $\text{Fe}_2\text{O}_3$  of DSF was found to be 84.81%. the loss on ignition of DSF was found to be 4.96% which is in compliance with upper limit prescribed in ASTM Standards C1240 (ASTM, 2004c). The silica content of DSF is in compliance with limits predefined by ASTM Standards C1240 (ASTM, 2004c) for use as constituent material in cementitious mixes.

The XRD of DSF is presented in Figure 3. The XRD pattern obtained indicates a hump with no crystalline peak. Therefore, it can be concluded that the mineral composition of DSF, majorly silica, is amorphous in nature. Silicate minerals in their amorphous state are highly reactive with Portlandite mineral. This is indicative of a potential chemical interaction between silica compounds in DSF and Portlandite minerals in HCWA to form an additional secondary C-S-H gel at both early and later stages of hydration. An additional secondary C-S-H gel formed contributes towards the reduction of the Portlandite amounts and at the same time increases the quantity of the C-S-H gel. This results in an overall enhancement in the strength of hardened cement paste matrix.

### Aggregates

The fine aggregate used were locally sourced quartzitic natural river sand in uncrushed form. They tested with specific gravity of 2.83 and maximum aggregate size of 5 mm. These fine aggregates were washed to remove their clay content and dried to a saturated surface dry condition prior to use as constituent material in mortar

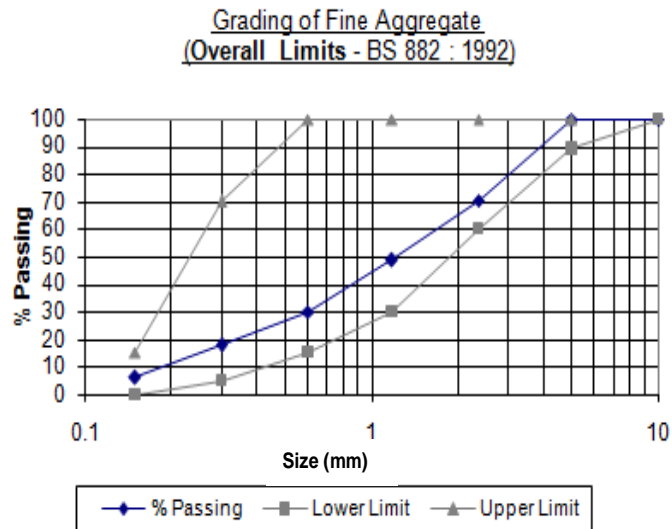


Figure 4. Particle grading of fine aggregates.

mixes. They were graded in accordance to BS812: Part 102 (BSI, 1989) and the grading of fine aggregates used was in compliance with the overall grading limits of BS 882 (BSI, 1992) as shown in Figure 4. The fineness modulus of the fine aggregates was determined to be 3.26.

### Superplasticizer and mixing water

An aqueous solution of polycarboxylic ether by the commercial designation of Glenium Ace 388 was used as a superplasticizer in this study. The superplasticizer was incorporated into the mortar mixtures at a required dosage in order to maintain a desired level of workability. Potable water from a local water supply network was used as the mixing water for all mortar mixes produced.

## METHODS

### Characterisation of binder materials

The chemical compositions of HCWA, DSF and PC were determined by X-ray fluorescence analytical method using an X-ray spectrometer with the commercial name "Rigaku", RIX3000. Mineral phases of oxide compounds detected by X-ray fluorescence analysis were identified by the X-ray diffraction method using a Bruker X-ray diffractometer. Analysis of the XRD was performed for the determination of mineral phases using the fingerprint method (Whitfield and Mitchell, 2008). The loss on ignition (LOI) of the materials was determined in accordance to the procedures prescribed in the ASTM Standard C311 (ASTM, 2004a).

Particle size distribution, median particle size diameter ( $d_{50}$ ) and specific surface area of the powders were determined by laser diffraction analysis using a Malvern laser particle size analyzer. Applicability of the laser diffraction technique as an alternative to the conventional Blaine permeability method for the determination of specific surface area of cementitious materials was verified by previous research (Frías et al., 1991). Specific gravity values of the samples were determined using a Le Chatelier flask and the procedures prescribed in ASTM Standard C188 (ASTM, 1995). Kerosene was used as liquid medium for the assessment of the specific gravity to avoid hydration of test samples during the test.

**Table 2.** Proportion of constituent materials and rheological properties of mortar mixes.

Batch designation	% DSF	%HCWA	Combined cement replacement (%)	Cement	DSF	HCWA	Sand	Water	SP dosage (%)	w/c	Mortar flow (%)	Slump (mm)	Bulk density (kg/m <sup>3</sup> )
				------(kg/m <sup>3</sup> )-----									
C	0.0	0.0	0.0	708	0	0	1593	227	0.40	0.32	26.70	50	2246
CS	7.5	0.0	7.5	655	53	0	1593	227	1.00	0.32	30.20	60	2230
W4	7.5	4.0	11.5	627	53	28	1593	227	1.10	0.32	26.40	50	2200
W6	7.5	6.0	13.5	612	53	42	1593	227	1.30	0.32	26.60	65	2204
W8	7.5	8.0	15.5	598	53	57	1593	227	1.40	0.32	26.90	85	2214
W10	7.5	10.0	17.5	584	53	71	1593	227	1.50	0.32	30.90	50	2217
W12	7.5	12.0	19.5	570	53	85	1593	227	1.70	0.32	22.50	50	2193
W16	7.5	16.0	23.5	542	53	113	1593	227	2.60	0.32	38.20	90	2246

#### Standard consistency, initial and final setting times of blended cement pastes

For the purpose of determining the standard consistency, initial and final setting time of HCWA-DSF ternary blended cement, blended cement pastes containing 7.5% of DSF and HCWA content of 0, 4, 6, 8, 10, 12 and 16% by total binder weight were examined. Water content of the cement pastes was adjusted to yield a standard level of consistency as defined in BS EN 196-3 (BSI, 2005). Standard consistencies of the cement pastes were recorded as the ratio of water required to produce paste at a standard consistency by total cement weight. The initial and final setting times of blended cement paste was determined in accordance to procedures prescribed in BS EN 196-3 (BSI, 2005) using a manual vicat apparatus.

#### Design of mortar mixes

The binder: sand and water/binder ratios were maintained constant at 1:2.25 and 0.32 respectively for all mortar mixtures cast. The Portland cement binder was partially replaced using HCWA at substitution levels of 0, 4, 6, 8, 10, 12 and 16% by total binder weight. Meanwhile, DSF was used as a partial cement replacement material at a constant replacement level of 7.5% for all mixes containing HCWA. Superplasticizer was dosed at appropriate dosages to maintain the desired mortar slump of 70±20 mm, as prescribed in BS EN 206: Part 1 (BSI, 2000) as S2 (medium workability) slump range. A flow of mortar mixes was maintained within the range of 26±5% to ensure an

adequate workability of the mix for proper compaction within the steel moulds. The mix design of the control mortar mix (C) was performed using an absolute volume method prescribed in design code ACI 211.1 (ACI, 2000) to achieve a compressive strength of 50 MPa at the age of 28 days. PC was used as the only hydraulic binder in the control mortar mix (C). The composition of mortar mixes are summarised in Table 2.

#### Mortar mixing and curing

Each batch of mortar was produced using an epicyclic type mechanical mixer complying with specifications in ASTM Standard C305 (ASTM, 1994). During mixing of mortar mixes containing HCWA in partial substitution of Portland cement, HCWA, DSF and Portland cement were initially dry mixed at low mixing speeds for 3 min prior to the addition of other constituent materials. Further mixing sequences and durations were performed in accordance to standard procedures prescribed in ASTM Standard C305 (ASTM, 1994). After casting, the specimens were wrapped in wet jute bags for curing for 24 h prior to demoulding. After demoulding, specimens were cured for 28 days in a potable water tank where the ratio of the volume of curing water to the volume of specimens was kept low (around 0.48) (Hossain, 2006).

#### Rheological properties tests

An ASTM flow test was performed on fresh mortar mixtures

using flow tables complying with specifications prescribed in ASTM Standard C230 (ASTM, 1997b) and standard testing procedures described in ASTM Standard C109 (ASTM, 1998). Slump values of the mortar mixes were determined by a slump test performed in accordance to the procedures prescribed in BS 1881: Part 102 (BSI, 1983a). Fresh mortar flow and slump values obtained are presented in Table 2.

#### Compressive strength and bulk density tests

Mortar cube specimens with edge dimensions of 50 mm were moulded, cured and tested in accordance to the procedures described in ASTM Standard C109 (ASTM, 1998) for determining compressive strength of the hardened mortar mixtures produced. All mortar specimens fabricated were cured in lime saturated water for durations of 3, 7 and 28 days prior to being tested. The reported compressive strengths at their given ages were the average of three number of specimens tested. Bulk densities of hardened mortar mixtures were determined in accordance to methods in BS 1881: Part 114 (BSI, 1983b).

#### Chloride profiling test

For the purpose of the chloride profiling test, one prism specimen with the dimensions of 100x100x500 mm was fabricated from each mix design stated earlier. The mortar prism was removed from the mould after 24 h from the

**Table 3.** Standard consistency, initial setting time and final setting time of blended cement pastes.

Cement paste designation	Portland cement content (% by total binder's weight)	DSF content (% by total binder's weight)	HCWA content (% by total binder's weight)	Standard consistency	Initial setting time (min)	Final setting time (min)
CP	100	0	0	0.29	131	218
CSP	92.5	7.5	0	0.31	144	240
W4P	88.5	7.5	4	0.32	200	339
W6P	86.5	7.5	6	0.32	198	336
W8P	84.5	7.5	8	0.32	196	330
W10P	82.5	7.5	10	0.32	154	222
W12P	80.5	7.5	12	0.32	154	230
W16P	76.5	7.5	16	0.33	155	297

initiation of mixing and water cured for a total duration of 28 days. Then, the mortar prism was removed from the curing tank and immersed into salt water with constant sodium chloride concentration of 4%, totally immersed for 28 days. At the end of the immersion period, the mortar prism was removed from the salt water and dried. Two numbers of mortar cylinders with a diameter of 25 mm and a length of 100 mm were extracted from the mortar prism using a steel core cutter. The extracted cylindrical mortar specimens were then cut into discs to a thickness of 10 mm and ground to a fine powder using a ring mill whereby 100% of the sample passes the 150  $\mu\text{m}$  dry sieve. The chloride content of each disc was determined in accordance to procedures detailed in BS 1881: Part 124 (BSI, 1988).

In a non-steady state of chloride diffusion which normally happens in structural concrete, the activity of chloride diffusing through concrete or mortar varies. This occurs with the distances along the sections perpendicular to the direction of chloride diffusion. Under such circumstances, Fick's Second Law of Diffusion is applicable to estimate the diffusion coefficient of chloride ions through the concrete material. Fick's Second Law of Diffusion is expressed in the second degree partial differential equation as shown in Equation 1.

$$\frac{\partial C^2}{\partial t^2} = D \frac{\partial^2 y}{\partial x^2} \quad (1)$$

Equation 1 is solved by applying initial and final boundary conditions as follows:

$C = 0$  at  $x > 0$  and  $t > 0$  [Initial boundary condition]

$C = C_0$  at  $x = 0$  and  $t > 0$  [Final boundary condition]

By solving partial differential equation in Equation 1, the following solution can be obtained and used for the calculation of diffusion coefficient of each layer tested:

$$C(x, t) = C_0 \left\{ 1 - \operatorname{erf} \frac{x}{\sqrt{4Dt}} \right\} \quad (2)$$

where,  $C_0$  is the chloride content at the datum layer (taken as first layer tested) (%);  $\operatorname{erf}$ , is the error function;  $C(x, t)$ , is the chloride concentration at a given depth  $x$  (in cm) (%);  $t$ , is the period of exposure (s);  $D$ , is diffusion coefficient ( $\text{cm}^2/\text{s}$ ).

## RESULTS AND DISCUSSION

### Standard consistency, initial and final setting times of high calcium wood ash (HCWA)-densified silica fume (DSF) blended cement pastes

The results of engineering parameters of HCWA-DSF blended cement pastes, namely, standard consistency along with their initial and final setting times are presented in Table 3. The addition of 7.5% DSF as a partial cement replacement material increased the water requirement of blended cement paste in order to achieve a standard degree of paste consistency. The inclusion of 4% HCWA by total binder weight resulted in DSF blended cement paste. This in turn, resulted in a marginal increase in water demand to achieve standard consistency. However, subsequent increments in the level of cement replacement by HCWA up to 12% by total binder weight did not have any further effect on water demands for the cement paste to achieve standard degree of consistency. The marginal effect of HCWA inclusion in cement on water demand to achieve a standard degree of consistency can be attributed to the similarity in particle grading between HCWA and Portland cement as presented in Figure 2.

The inclusion of HCWA at all levels of cement replacement adds up to 16% by total binder weight. This was observed to prolong the initial setting time as compared to pure cement paste (CP) and blended cement containing DSF (CSP). The most significant delay in initial setting of cement paste was noted when wood ash was used at 4% by total binder weight. In addition, the inclusion of HCWA at cement a replacement level between 4 to 8% in blended cement paste containing 7.5% DSF resulted in a delay of the final set as compared to the pure cement paste and the cement paste containing 7.5 % DSF. All HCWA-DSF blended cement pastes satisfied the requirement of ASTM C150 (ASTM, 1997a) requirements of 45 min initial minimal setting times and 365 min maximum final setting times. Cement paste CSP which has 7.5% by binder weight of DSF

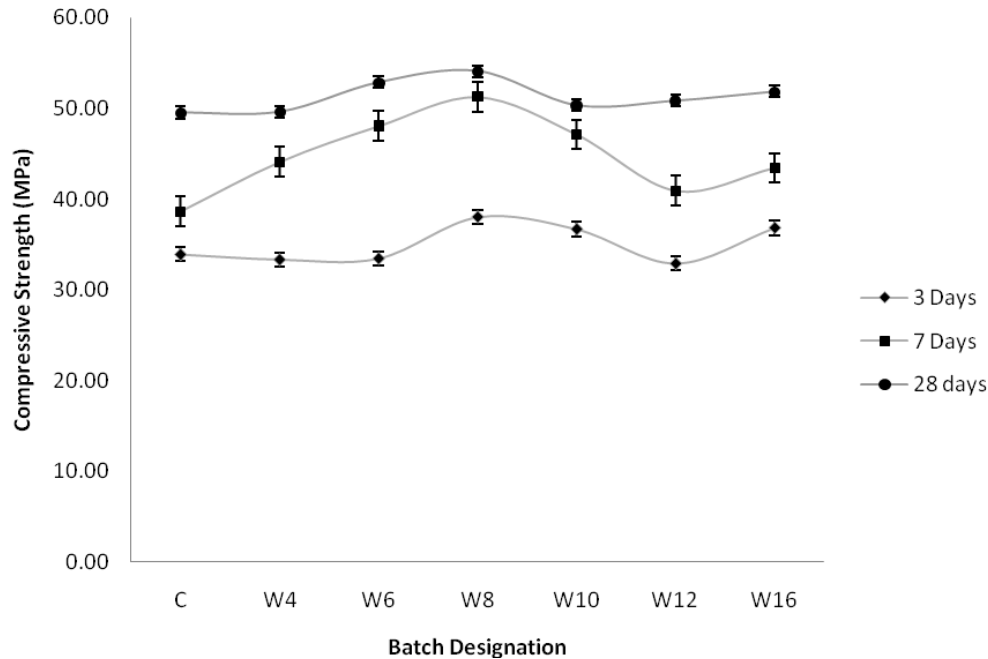


**Figure 5.** Variation in compressive strength at various replacement levels with HCWA.

showed a delayed initial and final set as compared to the pure cement paste CP. This is due to the clinker dilution effect which slowed down the rate of hydration resulting in prolonged setting times of paste (Elinwa and Eje, 2004). Further replacements of Portland cement with 4, 6 and 8% by weight of HCWA as in cement paste W4P, W6P and W8P resulted in further dilutions of Portland cement content, hence, further extensions of both initial and final setting times as compared to paste CSP. The observed increasing delays in setting times of the cement paste with an increasing replacement level with wood ash is consistent with the observations of other researchers (Elinwa and Eje, 2004; Elinwa and Mahmood, 2002; Udoeyo and Dashibil, 2002; Wang et al., 2008b). However, on further addition of HCWA at a dosage of 10% up to 16%, a significant reduction in both initial and final setting times could be observed. At these levels of cement replacement using HCWA, calcium carbonate mineral was present in quantities which are significant to accelerate the hydration of  $C_3S$  mineral of Portland cement (Ramachandran and Zhang, 1986) which offset the clinker dilution effect.

#### Superplasticizer requirement and workability of fresh mortar

The flow and slump values of fresh mortar produced along with their respective required dosage of superplasticizer to achieve a slump range of  $70 \pm 20$  mm are presented in Table 2. A significant rise of the required

dosage of superplasticizer from 0.4 to 1.1% was recorded upon the incorporation of DSF and HCWA as a supplementary binder at 7.5 and 4% respectively. The results also indicated that as the content of HCWA was increased from 4 to 12%, while DSF content was maintained at 7.5%, the required dosage of superplasticizer to maintain constant level of mix workability was increased gradually from 1.1 up to 1.7%. When the HCWA content was increased beyond 12% up to 20% by total binder mass, no significant increase in dosage of superplasticizer required to maintain a constant level of workability was observed. Generally, with the combined inclusion of DSF and HCWA as a supplementary binder material, the slump and flow of mortar mixes could be maintained at a given level with a minor adjustment to the dosage of superplasticizer incorporated into the mix.

#### Bulk density and compressive strength of hardened high calcium wood ash (HCWA)-densified silica fume (DSF) cement mortar

Bulk densities of hardened mortar are presented in Table 2. Generally, it was observed that the inclusion of HCWA as a supplementary binder in mortar had resulted in a marginal reduction of the bulk density of mortar mixes produced with reference to the control mortar (C).

Figure 5 indicates the compression strength with 95% confidence intervals calculated from the pooled standard deviations and the replicates of each mix at specimen ages 3, 7 and 28 days. At the age of 3 days, the average

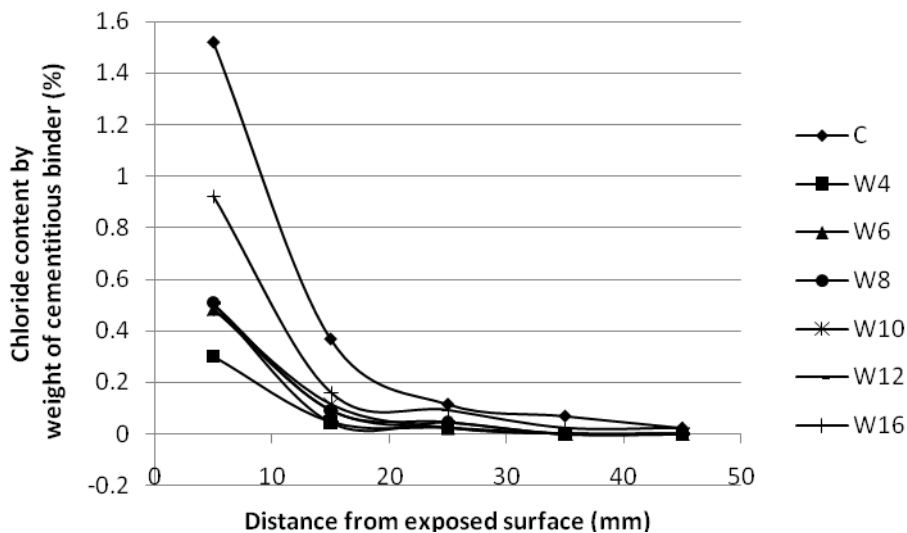


Figure 6. Chloride content profile of mortar mixes.

compressive strengths of mortar mixes C, W4, W6, W8, W10, W12 and W16 were determined as 33.9, 33.4, 33.5, 38.0, 36.7, 32.9 and 36.8 MPa respectively. The compressive strength of mortar W4, W6 and W12 was found to be marginally lower but still within the 95% confidence interval of the compressive strength for the control mortar (C). The trend observed is probably attributed to the dominating effect of dilutions in cement content of mixes containing HCWA and DSF. At the same age, mortar mixes W8, W10 and W16 was found to have a significantly higher compressive strength as compared to the control mortar.

At day 7, compressive strengths of mortar mixes C, W4, W6, W8, W10, W12 and W16 were determined as 38.4, 44.1, 48.0, 51.2, 47.1, 40.9 and 43.4 MPa, respectively. It can be noted that the compressive strength of all HCWA mortar mixes was found to be within the 95% confidence interval or significantly higher as compared to the compressive strength of the control mortar after 7 days. The higher rate of strength gained in the HCWA-DSF mortar compared to the control mortar between 3 and 7 days was mainly attributed to the combined effect of an early pozzolanic reaction and accelerated hydration rate of  $C_3S$  in the presence of a calcium carbonate mineral (Kakali et al., 2000). The Portlandite mineral present in HCWA could initiate a pozzolanic reaction with a amorphous silica content of DSF at an early age of hydration. This could contribute to the higher yield of C-S-H crystals, denser cement paste matrix and the corresponding higher rate of early strength development.

At 28 days, the compressive strength of the control mortar (C), W4, W6, W8, W10, W12, W16 and W20 was found to be 49.5, 49.6, 52.9, 54.1, 50.3, 50.8, 51.8 and 48.1 MPa respectively. The compressive strengths of mortars containing various levels of cement replacement

using HCWA and a constant DSF content of 7.5% was found to exceed the target design compressive strength of 45 MPa. The mortar mixes could be classified as high strength mortar by definition of the ASTM Standard C387 (ASTM, 2004b). All mortar mixes containing HCWA and DSF exhibited a compressive strength which lies within the 95% confidence interval or higher than pure cement mortar.

The optimum content of HCWA to ensure the best compressive strength performance at all curing ages is 8% by total binder weight as shown in Figure 5. Beyond the optimum level of cement replacement and/or increasing dosage of HCWA in mortar caused a gradual decline in compressive strength from the optimum compressive strength.

#### Chloride profile of hardened high calcium wood ash (HCWA)-densified silica fume (DSF) cement mortar

The chloride content profile of all mortar mixes subjected to immersion in a 4% NaCl solution for a total duration of 28 days is presented in Figure 6. Generally, it was observed that the chloride content reduces while increasing the distance from the exposed surface for all mortar specimens tested. The average chloride content and the average chloride diffusion coefficient of various mortar mixes tested are summarized in Table 4. It was observed that the average chloride content of mortar mixes W4, W6, W8, W10, W12 and W16 is significantly lower as compared to the control mortar. Among the W-series mortars, W4 was found to have the lowest average chloride content at any depth from the surface of exposure. Meanwhile, the average chloride content in mixes W6, W8, W10 and W12 was determined to be similar with respect to one another. Though the average

**Table 4.** Average chloride content and average chloride diffusion coefficient of various mortar mixes.

Mix designation	Average chloride content (%)	Average diffusion coefficient, $D_{avg}$ ( $\times 10^{-7}$ cm <sup>2</sup> /s)
C	0.42	3.59
W4	0.07	1.83
W6	0.12	1.65
W8	0.13	2.02
W10	0.12	1.79
W12	0.12	1.84
W16	0.24	3.57

chloride content of mix W16 was determined to be highest among the W-series mixes, it is still significantly lower than average chloride content of the control mortar. In addition, the results of chloride profile analysis, as expressed in terms of average chloride diffusion coefficients, are indicative that mixes W4, W6, W8, W10, W12 and W16 have a lower degree of chloride diffusivity as compared to the control mortar mix.

The chloride ion resistance of concrete gives an indirect measure of its permeability and internal pore structure as more chloride ions pass through a more permeable concrete (Hossain, 2006). The reduction in the average chloride ions content in the HCWA-DSF mortars and corresponding lower chloride ion diffusivity is attributed to the refined micro-pore structure of a HCWA-DSF blended cement paste matrix. The refinement in the micro pore structure of a HCWA-DSF blended cement paste matrix is achieved by the micro-filler effect of DSF within inter-particle voids of cement particles. It was also noted to have a high pozzolanic activity of DSF in the cement matrix in the presence of a uniformly dispersed Portlandite mineral contributed by HCWA. In this case, a silica fume pozzolanic reaction seems to occur mainly in larger capillary pores which are present within the cement paste matrix rather than within paste-aggregate interface. This has a direct contribution towards the refinement of micro pore structures of a cement paste matrix, hence a reduction in chloride diffusivity of a blended cement paste matrix (Gleize et al., 2003).

## Conclusions

In reference to the results acquired throughout the laboratory investigation, the following conclusions can be derived:

1. The inclusion of HCWA in blended cement up to a cement replacement level of 16% marginally increases the water demand of paste in order to achieve a standard degree of consistency.
2. The use of HCWA in parallel with DSF as a partial cement replacement material in blended cement paste

significantly delays the initial and final set of the cement paste, hence, allowing prolonged durations for compaction and placement.

3. The presence of HCWA in a mortar mix at a replacement level beyond 8% contributed towards an enhancement rate of compressive strength gain at an early age of curing.
4. The optimum level of cement replacement with HCWA for the best compressive strength performance at all curing ages up to 28 days is 8% by total binder weight.
5. The use of HCWA at a cement replacement level up to 16% by total binder weight parallel with small amounts of DSF (7.5%) contribute towards the refinement in pore structure of a cement paste matrix, hence, reduces the chloride diffusivity of mortar mixes produced.

## ACKNOWLEDGEMENTS

The research study was jointly funded by University Sains Malaysia Fellowship Programme, University Sains Malaysia Research University Postgraduate Research Grant Scheme (USM-RU-PRGS) and Research Grant of the second author.

## REFERENCES

- ACI 211.1 (2000). Standard practice for selecting proportions for normal, heavyweight, and mass concrete.
- Antiohos S, Maganari K, Tsimas S (2005). Evaluation of blends of high and low calcium fly ashes for use as supplementary cementing materials. *Cem. Concr. Compos.*, 27(3): 349-356.
- Antiohos S, Papageorgiou A, Tsimas S (2006). Activation of fly ash cementitious systems in the presence of quicklime. Part II: Nature of hydration products, porosity and microstructure development. *Cem. Concr. Res.*, 36(12): 2123-2131.
- ASTM C305-1994 (1994). Practice for mechanical mixing of hydraulic cement pastes and mortars of plastic consistency.
- ASTM C188-1995 (1995). Test method for density of hydraulic cement.
- ASTM C150-1997 (1997a). Specifications for Portland cement.
- ASTM C230-1997 (1997b). Specification for flow table for use in tests of hydraulic cement.
- ASTM C109-1998 (1998). Test method for compressive strength of hydraulic cement mortars (Using 2-in. or [50-mm] cube specimens).
- ASTM C311-2004 (2004a). Test method for sampling and testing fly ash or natural pozzolans for use in Portland cement concrete.
- ASTM C387-2004 (2004b). Specification for packaged, dry, combined materials for mortar and concrete.

- ASTM C1240-2004 (2004c). Standard specification for silica fume used in cementitious mixtures.
- BS 1881: Part 102 (1983a). Testing concrete. Method for determination of slump.
- BS 1881: Part 114 (1983b). Testing concrete. Methods for determination of density of hardened concrete.
- BS 1881: Part 124 (1988). Testing concrete. Methods for analysis of hardened concrete.
- BS812: Part 102 (1989). Testing aggregates. Method for sampling.
- BS 882 (1992). Specification for aggregates from natural sources for concrete.
- BS EN 206: Part 1 (2000). Concrete. Specification, performance, production and conformity.
- BS EN 196: Part 3 (2005). Methods of testing cement. Determination of setting time and soundness.
- Dwivedi VN, Singh NP, Das SS, Singh NB (2006). A new pozzolanic material for cement industry: Bamboo leaf ash. *Int. J Phys. Sci.*, 1(3): 106-111.
- Elinwa AU, Ejeh SP (2004). Effects of incorporation of sawdust incineration fly ash in cement pastes and mortars. *J. Asian Arch. Build. Eng.*, 3(1): 1-7.
- Elinwa AU, Ejeh SP, Mamuda AM (2008). Assessing of the fresh concrete properties of self-compacting concrete containing sawdust ash. *Construct. Build. Mater.*, 22: 1178-1182.
- Elinwa AU, Mahmood YA (2002). Ash from timber waste as cement replacement material. *Cem. Concr. Compos.*, 24: 219-222.
- Frías M, Sánchez de Rojas MI, Luxán MP, García N (1991). Determination of specific surface area by the laser diffraction technique. Comparison with the Blaine permeability method. *Cem. Concr. Res.*, 21(5): 709-717.
- Gleize PJP, Müller A, Roman HR (2003). Microstructural investigation of a silica fume-cement-lime mortar. *Cem. Concr. Compos.*, 25(2): 171-175.
- Hossain KMA. (2006). Deterioration and corrosion in scoria based blended cement concrete subjected to mixed sulfate environment. *Int. J. Phys. Sci.*, 1(4): 163-174.
- Kakali G, Tsivilis S, Aggeli E, Bati M (2000). Hydration products of C3A, C3S and Portland cement in the presence of CaCO<sub>3</sub>. *Cem. Concr. Res.*, 30(7): 1073-1077.
- Kolip A, Savas AF (2010). Energy and exergy analyses of a parallel flow, four stage cyclone precalciner type cement plant. *Int. J. Phys. Sci.*, 5(7): 1147-1163.
- Lothenbach B, Le Saout G, Gallucci E, Scrivener K (2008). Influence of limestone on the hydration of Portland cements. *Cem. Concr. Res.*, 38(6): 848-860.
- Naik TR, Kraus RN, Siddique R (2003). CLSM containing mixtures of coal ash and a new pozzolanic material. *ACI Mater. J.*, 100(3): 208-215.
- Poppe AM, De Schutter G (2005). Cement hydration in the presence of high filler contents. *Cem. Concr. Res.*, 35(12): 2290-2299.
- Rajamma R, Ball RJ, Tarelho LAC, Allen GC, Labrincha JA, Ferreira VM (2009). Characterisation and use of biomass fly ash in cement-based materials. *J. Hazard. Mater.*, 172(2-3): 1049-1060.
- Ramachandran VS, Zhang CM (1986). Influence of CaCO<sub>3</sub> on hydration and microstructure characteristic of C<sub>3</sub>S. *II Cemento.*, 83: 129-152.
- Udoeyo FF, Dashibil PU (2002). Sawdust ash as concrete material. *J. Mater. Civ. Eng.*, 14(2): 173-176.
- Udoeyo FF, Inyang H, Young DT, Oparadu EE (2006). Potential of wood waste ash as an additive in concrete. *J. Mater. Civ. Eng.*, 18: 605-611.
- Vassilev SV, Baxter D, Andersen LK, Vassileva CG (2010). An overview of the chemical composition of biomass. *Fuel*. 89(5): 913-933.
- Wang S, Llamazos E, Baxter L, Fonseca F (2008a). Durability of biomass fly ash concrete: Freezing and thawing and rapid chloride permeability tests. *Fuel*, 87(3): 359-364.
- Wang S, Miller A, Llamazos E, Fonseca F, Baxter L (2008b). Biomass fly ash in concrete: Mixture proportioning and mechanical properties. *Fuel*. 87(3): 365-371.
- Whitfield P, Mitchell L (Eds.) (2008). *Phase Identification and Quantitative Method* (1 Ed.). West Sussex: John Wiley & Sons Ltd.
- Worrell E, Price L, Hendricks C, Meida LO (2001). Carbon Dioxide Emissions from the Global Cement Industry. *Annu. Rev. Energ. Environ.*, 26: 303-329.
- Yajun J, Cahyadi JH (2003). Effects of densified silica fume on microstructure and compressive strength of blended cement pastes. *Cem. Concr. Res.*, 33(10): 1543-1548.
- Yaprak H, Aruntas HY, Demir I, Simsek O, Durmus G (2011). Effects of the fine recycled concrete aggregates on the concrete properties. *Int. J. Phys. Sci.*, 6(10): 2455-2461.
- Ye G, Liu X, De Schutter G, Poppe AM, Taerwe L (2007). Influence of limestone powder used as filler in SCC on hydration and microstructure of cement pastes. *Cem. Concr. Compos.*, 29(2): 94-102.
- Zelic J, Krstulovic R, Tkalcec E, Krolo P (2000). Properties of Portland cement-limestone-silica fume mortars. *Cem. Concr. Res.*, 30(1): 145-152.